REPORT DOCUMENTATION PAGE

Form Approved
OMB No. 0704-0188

1. AGENCY USE ONLY (*Leave Blank*)	2. REPORT DATE	3. REPORT TYPE AND DATES COVERED
	1/23/97	Final Report, 7/23/96-1/23/97

4. TITLE AND SUBTITLE

Microcontamination Sensor for VLSI Semiconductor Manufacturing

5. FUNDING NUMBERS

Contract

DASG60-96-C-0170

6. AUTHOR(S)

Pajo Vujkovic-Cvijin

7. PERFORMING ORGANIZATION NAME(S) AND ADDRESS(ES)

Los Gatos Research
1685 Plymouth St., Suite 100
Mountain View, CA 94043

8. PERFORMING ORGANIZATION REPORT NUMBER

9. SPONSORING/MONITORING AGENCY NAME(S) AND ADDRESS(ES)

sponsored by: BMDO/IST STTR
managed by: US Army Space and Strategic Defense Command, Huntsville, Alabama

10. SPONSORING/MONITORING AGENCY REPORT NUMBER

11. SUPPLEMENTARY NOTES

n/a

12a. DISTRIBUTION/AVAILABILITY STATEMENT

[redacted]

12b. DISTRIBUTION CODE

13. ABSTRACT (*Maximum 200 words*)

Feasibility demonstration of a trace-level water vapor sensor has been performed in Phase I. The sensor is critically needed in semiconductor industry, where trace concentrations of water in highly reactive gases used in Very Large Scale Integration (VLSI) manufacturing decrease significantly the yield of IC chips produced. The sensor described is based on optical spectroscopy in the middle infrared region, and uses a novel laser source, based on nonlinear frequency conversion. In Phase I we have demonstrated both the feasibility of producing such a source (diode laser-pumped, room-temperature operation), and the feasibility of its application for sensitive frequency-modulation spectroscopy of water vapor in the middle infrared region. The results achieved open up the potential to develop a novel optical microsensor capable of reaching the required ultra-high detection sensitivity in a package suitable for use in industrial environments. During Phase I we have also formed a partnership with an instrument manufacturer, who will contribute matching funds for Phase II project, and who will manufacture the instrument in Phase III.

14. SUBJECT TERMS	15. NUMBER OF PAGES
microcontamination, VLSI, semiconductor processing equipment, laser spectroscopy, trace gas detection	19
	16. PRICE CODE

17. SECURITY CLASSIFICATION OF REPORT	18. SECURITY CLASSIFICATION OF THIS PAGE	19. SECURITY CLASSIFICATION OF ABSTRACT	20. LIMITATION OF ABSTRACT

2. Table of Contents

3. Phase I Results Executive Summary

A trace level (ppb- and sub-ppb) water vapor sensor is critically needed in semiconductor manufacturing, where water vapor contamination present in reactive gases decreases significantly the yield of IC chips produced by very-large-scale integration (VLSI) and ultra-large-scale integration (ULSI) techniques. Los Gatos Research is developing a novel optical microsensor based on wavelength-modulation diode-laser spectroscopy in the middle infrared (2-5μm) spectral region (MIR). The MIR source is based on nonlinear optical frequency conversion of near-infrared diode laser radiation by using microstructured lithium niobate ($LiNbO_3$).

The feasibility of the proposed MIR laser source, as well as the feasibility of application of this source for ultrasensitive spectroscopic H_2O detection, has been demonstrated in Phase I of this project through the accomplishment of the following goals:

(1) a novel source of middle-infrared radiation based on difference frequency generation in bulk periodically poled $LiNbO_3$ (PPLN), pumped by diode lasers, has been designed and built;
(2) difference frequency generation at 2.6μm has been demonstrated with the normalized generation efficiency reaching 90% of the theoretically predicted value for bulk PPLN;
(3) H_2O spectroscopy was performed in the 2.6μm spectral region and detection sensitivity was measured. The parameters obtained with the feasibility demonstration apparatus provide the basis to determine the ultimate sensitivity of the final version, to be built in Phase II.

Fig. 1. presents the results of the H_2O detection sensitivity measurements, showing the minimum concentration detectable with the Phase I apparatus of 43 ppb·m of path-integrated concentration of low total pressure H_2O. This preliminary detection sensitivity, achieved with the Phase I apparatus, is already low enough to be useful for a number of applications. Within the Phase I effort, we have also developed the design of the Phase II version of the entire sensor system, including the middle-infrared radiation source (the most critical component), which would bring the detection sensitivity to sub-ppb levels reliably in Phase II. The block diagram of the sensor system, packaged for industrial use, is presented on Fig. 2.

The sensor described here represents an enabling technology for ULSI semiconductor chip manufacturing, where microcontamination control is imperative for high yield chip production to be attained.

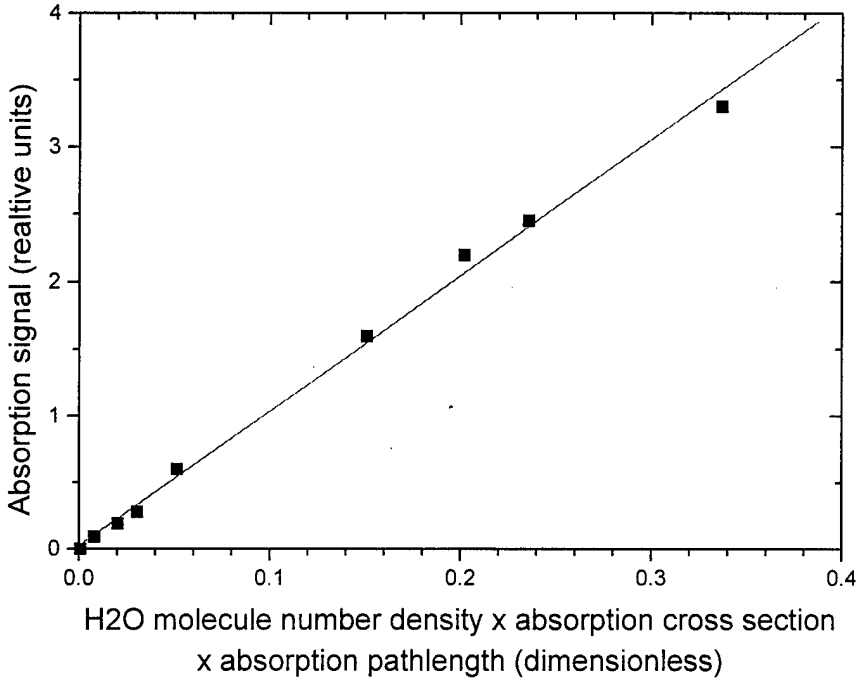

Figure 1 H_2O detection sensitivity measurements performed in Phase I.

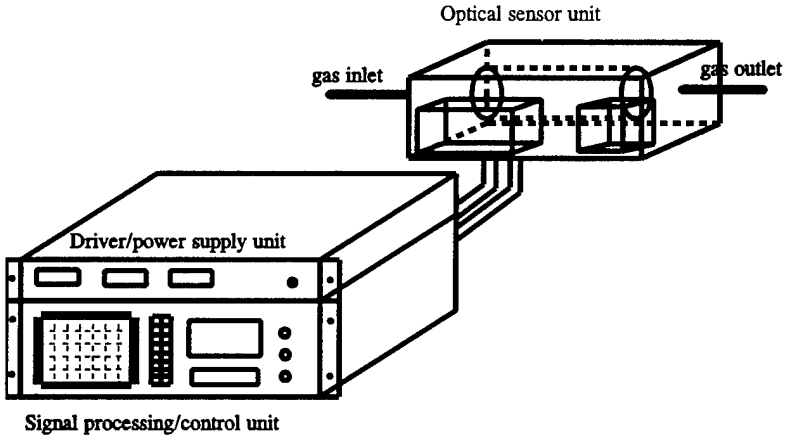

Figure 2. Water vapor microcontamination sensor packaged as a commercial product.

4. Introduction and Technical Background

A water vapor (H_2O) sensor capable of detecting ppb- and sub-ppb-level H_2O concentrations in corrosive gases is critically needed for microcontamination monitoring during the production of very-large and ultra-large-scale integration (VLSI and ULSI) silicon IC chips (e.g. microprocessors, memory chips). As the result of the corrosion in the processing equipment, originating from H_2O contamination, metal and metal-oxide particles are formed which contaminate and damage the IC chips under production, resulting in decreased yield of functional circuits. The problem becomes more severe as the scale of integration increases. As essentially all semiconductor manufacturers agree, the density of the upcoming circuits will make the problem acute. The instrument proposed here attempts to provide a solution to this problem.

The overlap of recent advances in nonlinear optics, semiconductor lasers, and integrated optics has created a unique opportunity for the development of a sensing instrument capable of detecting ppb-and sub-ppb-level trace concentrations of H_2O in highly reactive gases, such as HCl, BCl and others. The sensor is based on frequency-modulation diode-laser spectroscopy in the middle infrared spectral region (MIR). It uses a nonlinear frequency conversion technique to convert the near-infrared (NIR) radiation of common III-V diode lasers into an output in the middle-infrared region, where strong fundamental absorption bands of H_2O and other species exist. Due to the combination of high sensitivity, spectral selectivity-specificity, non-invasive monitoring and robust design, the performance of this sensor surpasses that of other diode laser-based sensors as well as Fourier-transform infrared (FTIR) gas detectors, whose application for this particular problem has been studied in the past.

The key component of the gas sensor proposed here is an MIR laser source in the 2.6μm spectral region. Existing diode lasers operating in the MIR have failed to reach the stage of wide practical applications, because they require cryogenic cooling and are fragile (lead-salt lasers). Pulsed optical parametric oscillators work at room temperature, but they are impractically large and expensive. Room-temperature diode lasers beyond the near-infrared (0.8 to 2μm) region are now under development (e.g. Sb-based quaternary diodes, quantum cascade diodes), but reliable, commercial-grade devices with a sufficiently wide tuning range are not likely to appear for years from now.

By combining the technologies of nonlinear optics, integrated optics and diode lasers, which are all currently available, it is now possible to develop a 2-5μm source which will have the properties required not only by the instrument described above, but by a number of other sensors. This source is based on difference frequency generation (DFG), also known as difference frequency mixing, in a material of high nonlinear optical coefficient. We propose here to develop a novel tunable MIR laser source pumped by two commercially available NIR lasers. The nonlinear interaction takes place in a periodically poled lithium niobate ($LiNbO_3$) crystal. The output beams of two NIR diode lasers of different frequencies are brought into interaction in

the crystal, modified by periodic poling in such a way to provide quasi-phase matching (QPM) for incident and generated fields. The difference frequency generation (DFG) effect produces a new light beam at a frequency equal to the difference between the frequencies of the input beams. The best material currently known to satisfy all the basic requirements (non-linear coefficient, durability, cost) for a DFG mid-infrared light source in the 2-5μm region is periodically poled lithium niobate (PPLN).

The properties of this microstructured material can be adjusted, using well-developed photolithographic techniques to meet the demands of a wide range of frequency-conversion applications.

Recent processing breakthroughs have made the wafer scale production of PPLN possible [1-3]. As a result of its patterned microstructure, PPLN material offers revolutionary improvements over the base lithium niobate material, including a) a fourfold improvement of the nonlinear coefficient, b) the elimination of photorefractive damage up to the damage threshold of the material, c) the flexibility to use an efficient phase matching process to produce tunable radiation from diode lasers at any wavelength between 350 nm in the ultraviolet and 5 μm in the infrared, and d) a fifty-fold broadening of the infrared thermal acceptance, making high-power infrared generation possible. This combination of characteristics gives PPLN a significant advantages over other nonlinear materials in this wavelength range such as KTP. Most significant, PPLN devices can be mass produced from inexpensive wafers, offering a potential cost below that of a semiconductor diode laser chip. The unique combination of high performance and low cost makes PPLN an ideal nonlinear material for frequency conversion applications.

During the Phase I we have eliminated the key technical risk by building and demonstrating a laboratory prototype of a room-temperature MIR diode laser source in the 2.6um spectral region, based on difference frequency generation. In this Phase II proposal we propose to develop the prototype of the complete sensor system for water vapor-contamination detection in corrosive gases. We have already identified a commercial partner who will contribute funding during the Phase II and who will take over instrument production and marketing. Other potential applications of the technology proposed here will also be considered. Because of the pressing need for this instrument which appears to exist within the semiconductor industry, we are planning an aggressive and intensive development effort aimed at achieving the level of beta-testing within six months after the end of Phase II.

We have pointed out in our Phase I proposal that the research proposed here originates from a real demand for this sensor which exists within the semiconductor industry, and that the market existence and size was well known. It turned out that during the Phase I project we had at least three companies interested in investing in our technology, with one (Delta F Corporation) clearly standing out with its background and experience. The ease with which we found a commercial partner for this endeavor demonstrates the market opportunity for the sensor proposed.

Both bulk and waveguide DFG has been demonstrated in QPM $LiNbO_3$ (PPLN) samples [4-7]. Although the highest conversion efficiencies have been demonstrated in waveguide structures, bulk PPLN offers the advantage of higher power handling capacity, simpler fabrication resulting in lower complexity and cost, reduced development risk, improved mechanical stability (lower sensitivity to misalignment) and capability for broad and easy wavelength tuning by simple variation of either the incident angle, the poling period or crystal temperature. The capability of the bulk-PPLN technology to conform to the requirements of an industrial-grade instrument and the maturity of supporting technologies has convinced us that DFG in bulk material is preferred solution over waveguide DFG for this application.

5. Degree to Which Phase I Objectives Have Been Met

As stated in our Phase I proposal, our main goal has been to demonstrate the feasibility of developing an ultrasensitive diode-laser based microcontamination sensor, specifically aimed at detecting trace-level water vapor concentrations. The main proposed innovation is a novel solid-state mid-infrared laser source based on III-V near-infrared laser diodes and nonlinear frequency conversion in bulk microstructured nonlinear material.

We quote here the Phase I objectives, as stated in our Phase I proposal [8]:

- **"Objective 1:** we will design a mid-infrared laser source based on III-V NIR diode lasers which uses QPM nonlinear frequency conversion in microstructured $LiNbO_3$.
- **Objective 2:** we will demonstrate mid-infrared light generation at the wavelength of 2.6μm by our device.
- **Objective 3:** perform absorption spectroscopy measurements on H_2O and estimate the detection limit."

All three objectives stated above have been met in our Phase I work. The following sections contain a detailed description of our experimental work and the results achieved.

6. Phase I Experimental Work and Results

6.1. Experimental apparatus

Laser sources selected to generate MIR radiation around 2.6μm were: (1) a tunable diode laser with nominal center wavelength of 750-760nm and (2) a cw Nd:YAG laser at 1064nm. This choice is based both on the current state of technology development of laser sources and on the cost considerations of commercial lasers. Both of these lasers are commercially produced in substantial quantities, which ensures both reliability resulting from mature technologies and acceptable cost, making them ideal for use in this case. Since the power generated in the DFG process is proportional to the product of powers of the two input lasers, the lasers selected represent a favorable choice also in the sense that the diode laser provides easy tunability and easy frequency modulation (by injection current), while the highly efficient Nd laser provides power (diode-pumped Nd laser is the workhorse of the laser industry and provides the best photon/$ ratio overall). Accordingly, the DFG process comes out with a source having all of these features: tunability in the MIR region, power, and acceptable cost.

We have investigated two types of diode lasers, both with output powers around 10mW: Sharp LTO31MD (750nm nominal center wavelength, Fabry-Perot cavity) and David Sarnoff Research Center CD1179A (760nm nominal center wavelength , distributed feedback cavity). The results with both lasers were essentially equivalent, with the reproducibility of the operating point (injection current, temperature) being much better with the distributed feedback (DFB) laser, as expected. Since the Phase I resources did not allow the purchase of new equipment, the cw Nd laser we used was an existing flashlamp-pumped Nd:YAG laser (CVI C-95), modified to provide a clean, linearly polarized, TEM_{00} mode with several tens of mW of output power. The output of this laser effectively mimics a diode-pumped unit. The resulting performance described here is completely analogous to the results that would have been obtained with an all-solid-state Nd laser.

Block diagram on Fig. 6.1 presents the layout of our system. The output beam of the diode laser was collimated (Melles-Griot f/8.0mm diode laser lens) and shaped by an anamorphic prism pair (Melles-Griot 4X anamorphic prisms). The beam was subsequently compressed by a 7:1 inverted beam expander (off-the-shelf NIR coated plano-convex lenses), in order to generate a beam of approximately the same propagation parameters as the Nd laser beam. The two beams were combined by a dichroic beam-splitter (Omega Optical 880DLRP/9641) and focused by a NIR coated 60mm focal length lens into the PLLN crystal. The position of the diode beam focus was axially adjustable in order to compensate for the chromatic aberration in the focusing lens and the $LiNbO_3$ crystal. The optical system was designed to create overlapping beam waists of <100μm diameter for each beam; experimental investigation with a CCD camera imaging system confirmed these values and was also used as an aid in initial alignment. Since it turned out to be easy to achieve the initial alignment, later alignments were done by an IR sensitive card only, followed by corrections to maximize the DFG power on the InAs detector.

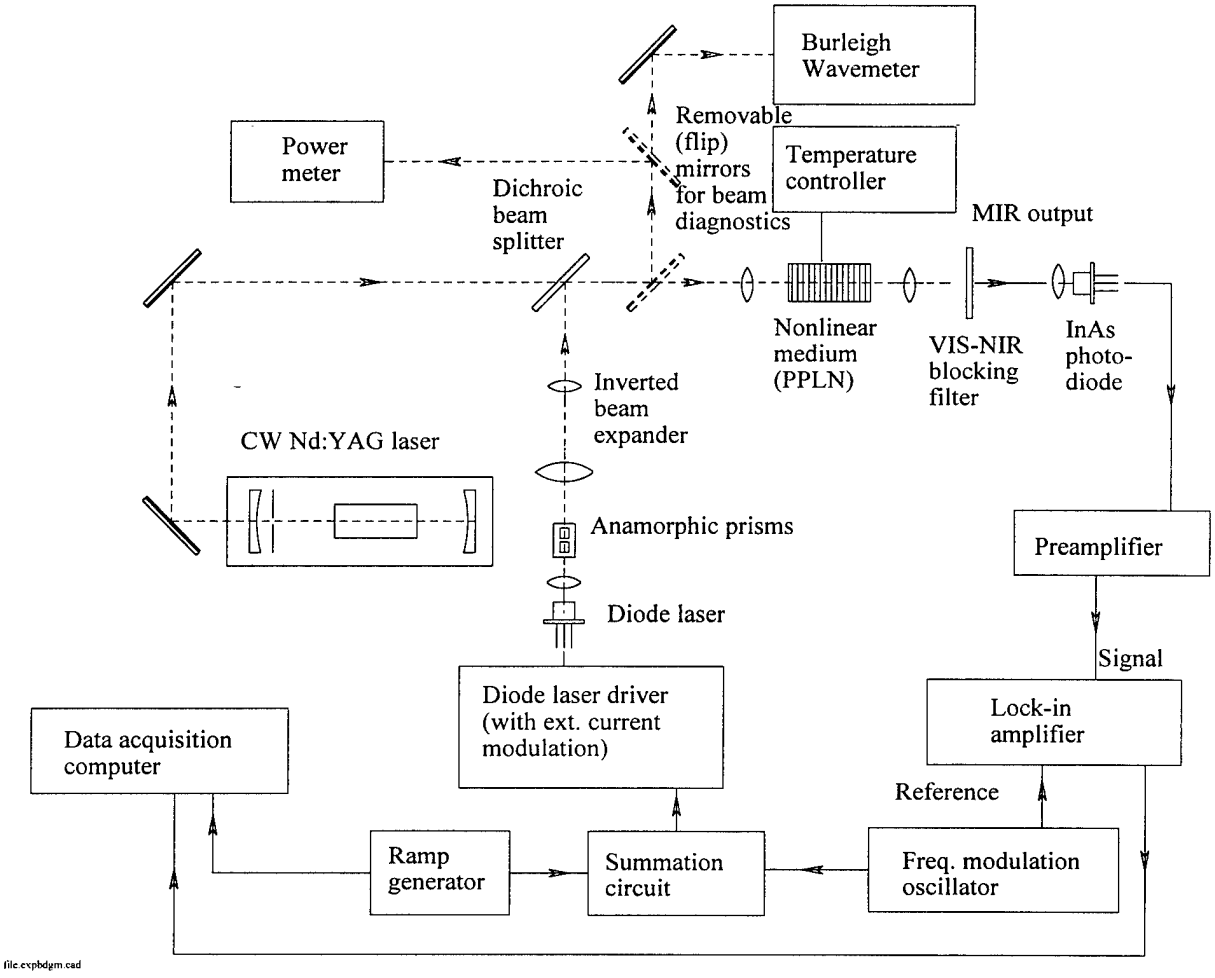

Fig. 6.1.Block diagram of the Phase I experimental apparatus.

We have incorporated two removable (flipping) mirrors in the setup (Fig.6.1) to provide for the power (Laser Science power meter) and wavelength (Burleigh WA-20 wavemeter) diagnostics. The PPLN crystal (Crystal Technology, Palo Alto) was 6mm long and poled with 21.0μm period. The crystal, placed on top of a small thermoelectric (Peltier) element for temperature control (acting under a Melles-Griot 06DLD203 driver), was held by an xyzϕ mount. The output MIR beam was recollimated by a ZnSe lens. After filtering out the residual 760nm and 1064nm radiation by a germanium filter, the beam was focused by another ZnSe lens onto an InAs detector (EG&G Judson J-12).

The diode laser injection current and temperature stabilization was provided by a Melles-Griot 06DLD103 diode laser driver, which has the provision for external injection current modulation. The frequency (wavelength) modulation was achieved by a Hewlett-Packard 3336 synthesizer (oscillator, Fig.6.1). The waveform which provides wavelength "sweeping" across the absorption peak was of triangular (ramp) shape produced by a Stanford Research Systems DS340 waveform synthesizer. The two waveforms (modulation and sweeping) were superimposed and input to the diode laser driver. The preamplified (Judson 700F preamp) signal from the InAs detector was measured by a lock-in amplifier (Stanford Research Systems 510), referenced to the modulation signal. The output of the lock-in amplifier was digitized by a fast A/D convertor (National Instruments PC-TIO-10) controlled by a data acquisition computer (IBM PC compatible), operating under LabWindows software (Fig. 6.1).

6.2. Experimental results

6.2.1. Difference-frequency MIR beam generation

The Nd:YAG laser used was a free-running laser with no axial mode control. The bandwidth of the laser is not as narrow as is the case with single longitudinal mode lasers. In order to compare our results with published data, we will normalize the DFG efficiency calculations accordingly. The Nd laser was intentionally operated with high intracavity losses, so that only a few axial modes had enough amplification to raise above the threshold, and the bandwidth remained relatively small. Measurement of laser's bandwidth with a laser spectrum analyzer (in the low resolution mode) revealed the bandwidth of 2.50GHz ($0.083cm^{-1}$, 0.0094nm). Within that bandwidth, the laser's output was 100mW, of which 80mW reached the PPLN crystal, of which only a certain portion, which spectrally overlaps with the diode laser output, as described below, contributes to DF generation.

The diode lasers used in the experiments delivered up to 7mW of 760nm radiation. The spectral bandwidth was ~100MHz. Typically, 4.9mW of 760nm power reached the PPLN crystal. After taking into account the spectral overlap factor of the two beams, which can be easily calculated, it was found that 5.0mW of 1064nm power contributed to the difference mixing process, i.e. approximately the same as the diode laser power. Relatively low power contributed by the Nd laser is by no means a limiting factor, as explained above, but is rather a

feature of the apparatus used for feasibility demonstration in this phase.

The power generated in the DFG process was measured by a calibrated InAs photodiode (Judson J-12) and the losses on the blocking filter and other components in the beam's path (Fig. 6.1) were taken into account. Typically, the output power of 15nW at 2.6μm was produced by the experimental apparatus used in this study. By using the definition $\eta=P_{IR}/P_1P_2L$, where P_{IR} is the DFG output power, P_1 and P_2 are the pump powers, L is the crystal length, we calculate for the DFG efficiency the value of $\eta=1\cdot10^{-3}W^{-1}cm^{-1}$. Based on known parameters of $LiNbO_3$, conversion efficiency can be calculated from [5]. The resulting theoretically predicted efficiency is $\eta_{theor}=1.12\cdot10^{-3}W^{-1}cm^{-1}$, in close agreement with our experimental result. We attribute the achievement of such high conversion efficiency both to the quality of the PPLN sample, and, particularly, to the careful engineering of the beam delivery system, which provides good spatial overlap of two nearly diffraction-limited beams, tailored to have nearly identical propagation parameters.

At the level of sub-μW output powers demonstrated here, the signal-to-noise ratio (SNR) of the electronic detection process, limited by detector noise, affects the overall system sensitivity for trace gas detection. The Phase I experimental system described in this report demonstrates the feasibility of the technique, although not necessarily the full power available. The MIR output power is in our case limited by the performance (inadequate bandwidth) of the Nd:YAG laser used. Calculations of the signal-to-noise ratio corresponding to our signal power and the detection system noise, suggest approximately $SNR=10^3$ to be expected from the present setup.

6.2.2. Water vapor spectroscopy and detection

Second derivative wavelength-modulation spectroscopy was used to measure the absorption of water vapor samples in the 2.6μm spectral region. The goal of the project in Phase I was to demonstrate the detection capability and provide data for sensitivity calculations (see Phase I objectives above). Since the spectroscopy of H_2O in the visible through the mid-IR is extremely well known [9], we had plenty of reliable data on H_2O absorption line intensities, pressure broadening coefficients and their temperature and pressure dependencies to use in calculations and modeling of the H_2O spectrum. Based on these data, a very accurate information on the absorption of water vapor samples can be obtained and used as the input for sensitivity calculations. (The quantity termed "absorption" here is traditionally (in modulation spectroscopy) expressed as the dimensionless ratio of the absorption peak depth and baseline values, i.e. one minus transmittance. Another familiar related quantity is absorbance, which is the logarithm of base 10 of absorption). For the data analysis reported here, we have modeled H_2O absorption spectra by using the HitranPC software package developed at the University of Southern Florida and marketed by Ontar Corp. The spectral information database used was the 1992 (the latest) version of the HITRAN database, originally compiled by NASA [9].

Line intensities of H_2O absorption lines in the 2.6μm band are presented on Fig. 6.2.

Since the H_2O spectrum offers a wide range of absorption line intensities, which are accurately known, the task of absorption calibration of water vapor samples is made a lot easier than with other, less well-characterized gases. In fact, it is possible to look at more than 5 orders of magnitude wide range of absorption line intensities within the spectral range of just several cm^{-1}. This situation offers a unique opportunity for the study of H_2O detection sensitivity without the need to vary the concentration or pathlength in a wide range, but to make measurements on absorption lines of different (accurately known) intensities, whose lineshapes are also precisely known. Furthermore, since it is very difficult both to generate precise low concentrations of water vapor, and ensure that no contributions from the pathlength outside the sample cell are being measured, the results obtained by making measurements at various, including very small, line intensities are probably more reliable.

We have implemented this approach in the following way: a short pathlength samples of atmospheric water vapor were used. The diode laser was tuned to a strong, positively identified absorption line and the direct (no wavelength modulation, no second harmonic detection) transmission was recorded while the diode laser's wavelength was swept across the line. The result of this measurement, which together with known pathlength, temperature and total pressure yielded the water vapor concentration, was used as the input to the Hitran model. The Hitran model calculated first the H_2O content and, subsequently, the entire H_2O absorption spectrum in any spectral region. Weak absorption lines (for practical reasons, near the first strong line) were identified next, and their corresponding values of absorption for the given H_2O sample were determined from the Hitran model. Second harmonic wavelength modulation spectroscopy was applied to the selected lines and signal intensities measured. These signals corresponded to accurately known absorptions, which permitted the relationship between the signal and the absorption to be established. This relationship determined the sensitivity limit, the quantity we were measuring.

We have selected the spectral region around one of the strongest H_2O lines in the center of the band, at λ_c=2.665μm with the line intensity $S_c=2.18\cdot10^{-19}$ cm/molecule (Fig. 6.2). The parameters of this line are used in detection sensitivity calculations. However, at the pathlengths used in our measurements (between L=7.1cm and L=17.95cm) the intensity of this line is too strong at atmospheric concentrations to be useful for detection sensitivity measurements. For that reason, we have selected the following weaker lines in the vicinity of λ_c: λ_1=2.6640μm, $S_1=7.0\cdot10^{-21}$ cm/molecule; λ_2=2.6634μm, $S_2=5.1\cdot10^{-22}$ cm/molecule; λ_3=2.6628μm, $S_3=1.1\cdot10^{-21}$ cm/molecule whose positions and line intensities are presented on Fig. 6.3.

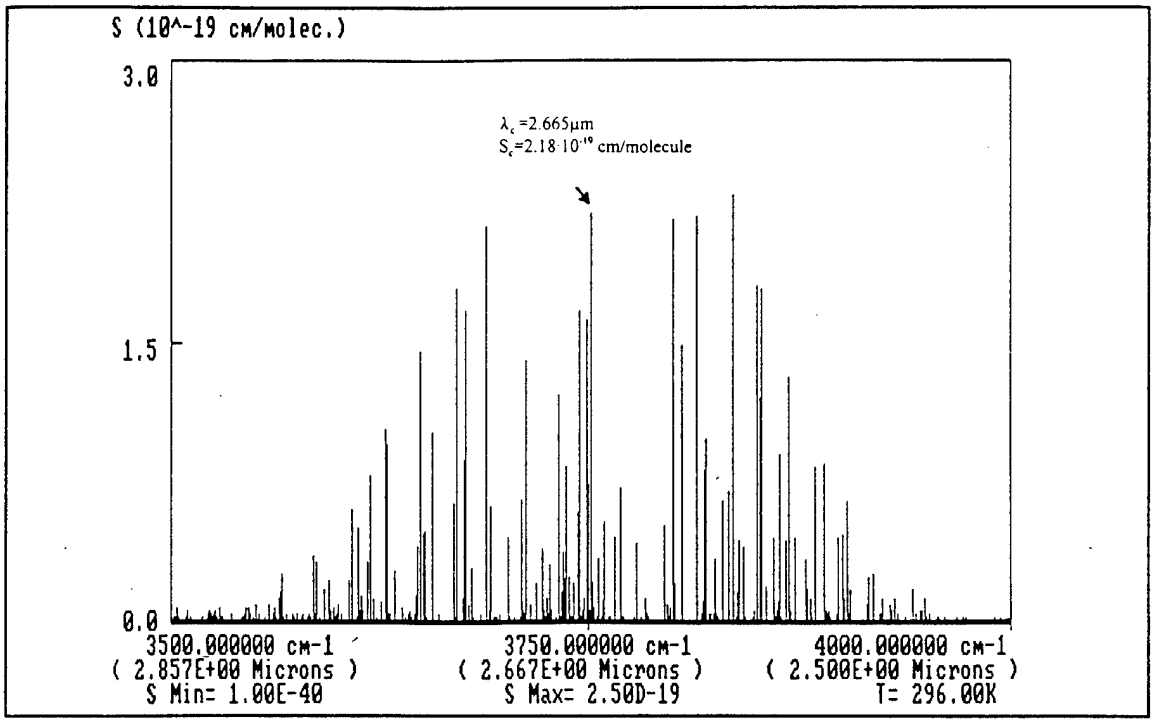

Fig. 6.2. Line intensities in the 2.6μm absorption band of H_2O. λ_c is the line referred to in the text.

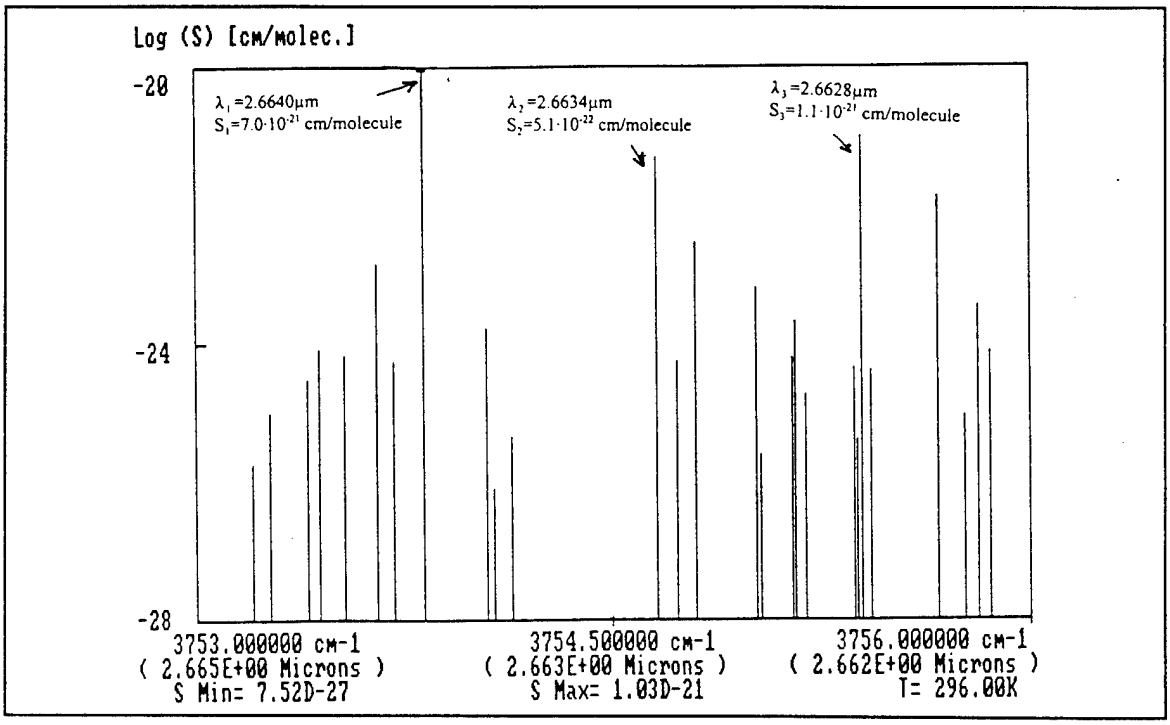

Fig. 6.3. Line intensities of selected lines. See text.

Fig.6.4. presents the result of direct absorption measurement of the relatively strong λ_1 =2.6640μm, $S_1=7.0\cdot10^{-21}$ cm/molecule H_2O absorption line. The horizontal axis shows the value proportional to the diode laser ramp current, which provides wavelength scanning across the region of the absorption line. This value is proportional to the source wavelength. We have modeled the measured spectrum in Hitran and obtained the synthetic spectrum of Fig. 6.5., where the positions and absorptions corresponding to two weaker lines λ_2 and λ_3 are also shown. These lines are in principle too weak to be measurable in direct absorption, but are detectable in second harmonic detection, as shown below. From the Hitran model, we have calculated the H_2O partial pressure to be 0.019 atm for this particular sample and determined the absorptions (one minus transmittance) for all three lines. Some of the results of second harmonic (second derivative) wavelength modulation spectroscopic measurements of these known absorptions are presented on Figs.6.6. and 6.7. Fig. 6.6. presents the second derivative of the strong λ_1 line from Figs. 6.4. and 6.5., corresponding to the absorption of A=0.2. Fig. 6.7 presents the same for the λ_3 line, with the absorption of $A=3.1\cdot10^{-3}$.

From the data of the type presented on Figs.6.4-6.7, we have constructed the diagram presented on Fig. 6.8. The interpolation of a linear relationship yields the sensitivity limit (for the signal-to-noise-ratio SNR=1) equal to $A_{min}=1.6\cdot10^{-3}$. This value agrees with the $SNR=10^3$ for the photon detection process estimated in Section 6.2.1.

7. Discussion and Conclusions

The feasibility of developing a room temperature diode laser-based source in the middle infrared, as well as the feasibility of using this source for spectroscopic H_2O detection, has been demonstrated. The preliminary detection sensitivity, characterized by minimum detectable absorption of $A_{min}=1.6\cdot10^{-3}$ is still impressive when normalized to a strong absorption line (λ_c =2.665μm from the previous section) and low-pressure pure H_2O (not atmospherically broadened). Absorption modeling by Hitran shows that the **minimum detectable absorption demonstrated corresponds to path-integrated H_2O concentration of 43 ppb·m.** This detection sensitivity already represents a respectable value. **With several meters folded pathlength, the capability to detect e.g. 10ppb level of H_2O would be a useful instrument for corrosive gas microcontamination analysis already.** In a corrosive gas environment, the existence of up to 1ppm of H_2O is thought to be quite common, although reliable numbers are hard to pin down, due to the lack of suitable instrumentation.

Based on experimental data presented in previous sections, the Phase I work can be summarized as follows:

(1) A novel source of middle-infrared radiation based on difference frequency generation in bulk periodically poled $LiNbO_3$ (PPLN) has been designed and built.

(2) Difference frequency generation at the wavelength of 2.6μm has been demonstrated; the normalized generation efficiency of $\eta=1\cdot10^{-3}W^{-1}cm^{-1}$ lies within 90% of the theoretically predicted value for bulk PPLN.

(3) H_2O spectroscopy was performed in the 2.6μm spectral region and detection sensitivity was measured. The parameters obtained with the feasibility demonstration apparatus provide the basis to determine the ultimate sensitivity of the final version, to be built in Phase II.

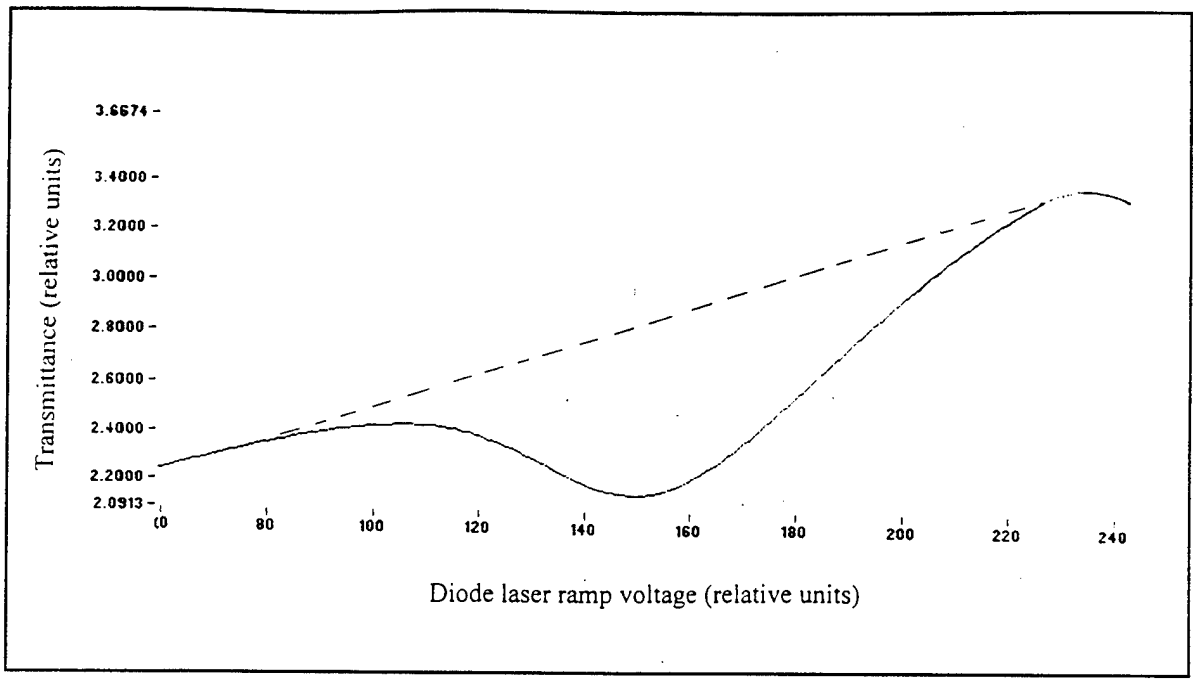

Fig. 6.4. Direct absorption measurement.

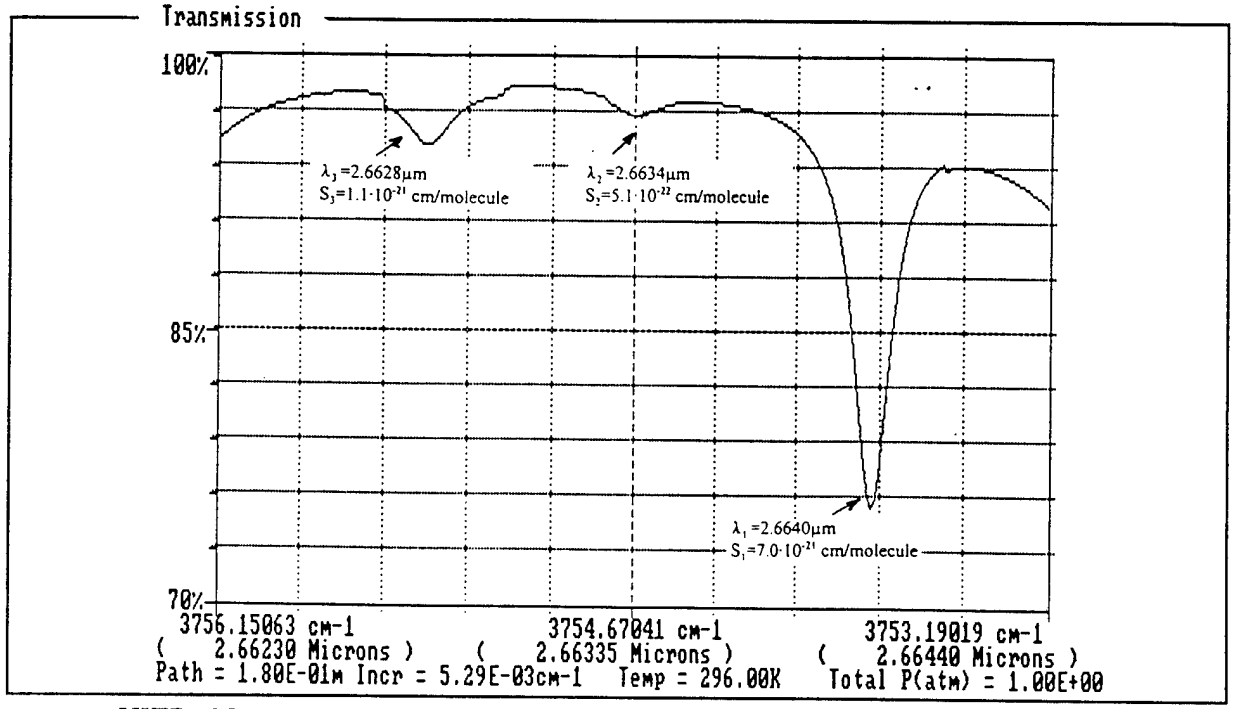

Fig. 6.5. HITRAN-generated synthetic spectrum

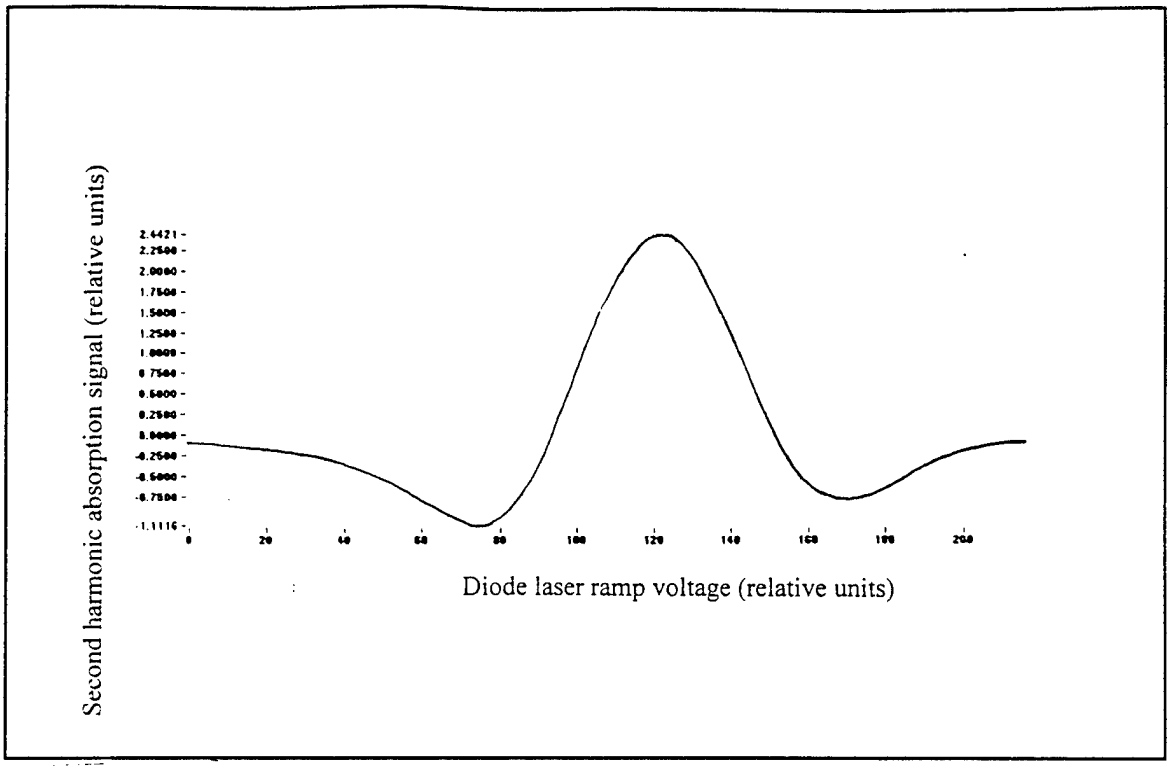

Fig. 6.6. Second harmonic absorption signal originating from a strong (λ_1, see text) line.

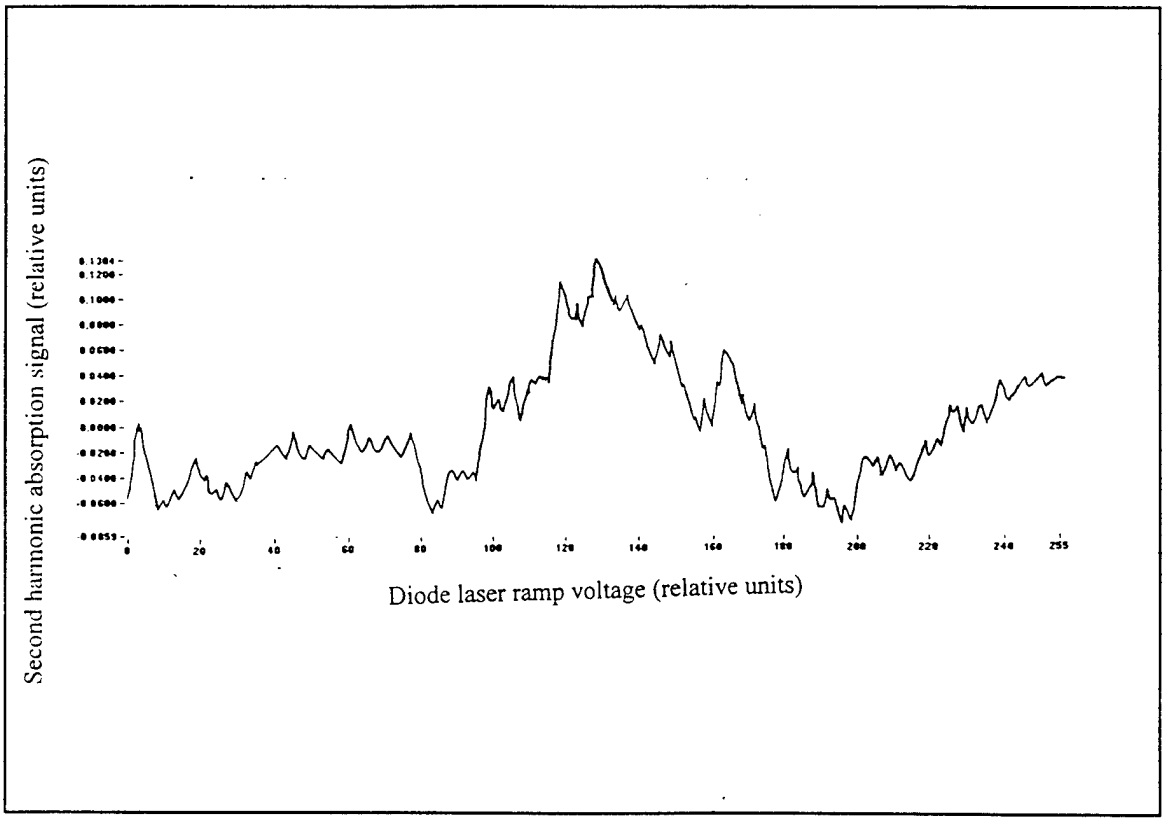

Fig. 6.7. Second harmonic absorption signal originating from a weak (λ_3, see text) line

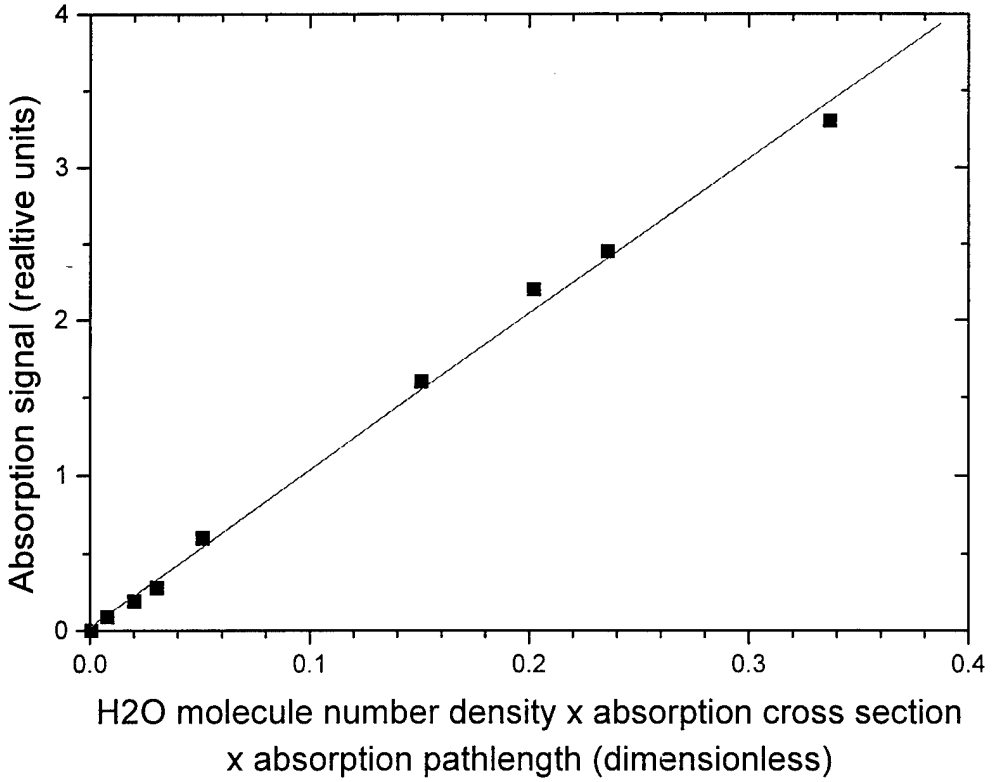

Fig. 6.8. H_2O detection sensitivity measurements performed in Phase I.

References

1. Fejer, M.M., *Nonlinear Optical Frequency Conversion.* Physics Today, 1994. **47**(5): p. 25-32.
2.Fejer, M.M., *et al.*, *Quasi-Phase-Matched Second Harmonic Generation: Tuning and Tolerances.* IEEE Journal of Quantun Electronics, 1992. **28**(11): p. 2631-2654.
3. Lim, E.J., *et al.*, *Infrared radiation generated by quasi-phase matched difference-frequency mixing in a periodically poled lithium niobate waveguide.* Applied Physics Letters, 1991. **59**(18): p. 2207-2209.
5. A. Balkrishnan et al., *"Broadly Tunable Laser-Diode Based Mid-Infrared Source"*, Opt. Lett. 21, 952 (1996)
6. L. Goldberg et al., *"Difference-Frequency Generation of Tunable Mid-Infrared Radiation"*, Opt. Lett. 20, 1280 (1995)
7. L. Goldberg et al., *"Wide Acceptance Bandwidth Difference Frequency Geneartion"*, Appl. Phys. Lett. 67, 2910 (1995)
8. P. Vujkovic-Cvijin, *"Microcontamination Sensor for VLSI Semiconductor Manufacturing"*, STTR Phase I, BMDO Contract # DASG60-96-C-0170.
9. Park, J.H. et al.,*" Atlas of Absorption Lines from 0 to 17900 cm^{-1} "*, NASA, 1987